

# How to get closer to reality in pressure test simulations with the SPH method

Martin Hušek, and Jiří Kala

**Abstract**—The article describes an algorithm for the generation of the spatial geometry of concrete based on a photograph, and its subsequent use in cylindrical pressure test simulations using the Smoothed Particle Hydrodynamics (SPH) method. The aim of the article is to present several simple steps of the algorithm which enable the achievement of variability in the results of simulated pressure load tests conducted on concrete. The main aim is to achieve the best possible match with reality. The fact is that during real load tests it is never possible to obtain two identical results, e.g. the same stress–strain curves for two concrete specimens. They will always differ slightly. However, this is inconsistent with what happens in the case of numerical simulations, where the result is always the same unless there is a change in the input values. The idea of the algorithm is thus to generate the spatial geometry of the structure of a material based on the utilization of a suitably selected and optimized noise function. In a cutting plane through its space, the noise function is visually identical to the photograph of the material. A unique result can be obtained with every additional photograph of the material. The structure generated in this way can be discretized advantageously using the SPH method while also incorporating numerical heterogeneity, which is used to enhance material heterogeneities, e.g. in the area where aggregate and cement binder are in contact. The article describes the whole procedure via an example of a cylindrical pressure test performed on concrete. The functionality of the algorithm is supported by simulation results.

**Keywords**—Concrete, heterogeneity, noise, Smoothed Particle Hydrodynamics.

## I. INTRODUCTION

THE complexity of computational models is constantly increasing. This phenomenon is not tied to certain fields of study – efforts to bring numerical simulations as close to reality as possible are visible everywhere, and civil engineering is no exception. When analyzing structures, the material model, the geometry and the boundary (and if needed, initial) conditions are all of importance. To a certain degree, the material model is related to the geometry or the scale at which the geometry is monitored. Why? The modeling of a heterogeneous material,

This outcome has been achieved with the financial support of the project GACR 17-23578S “Damage assessment identification for reinforced concrete subjected to extreme loading” provided by the Czech Science Foundation, and also with the support of the project FAST-J-17-4264 “Experimental and numerical verifications of meshfree methods in cases of dynamically loaded concrete structures” provided by the Brno University of Technology fund for specific university research.

M. Hušek is with the Faculty of Civil Engineering, Institute of Structural Mechanics, Brno University of Technology, Czech Republic (email: husek.m@fce.vutbr.cz).

J. Kala is with the Faculty of Civil Engineering, Institute of Structural Mechanics, Brno University of Technology, Czech Republic (email: kala.j@fce.vutbr.cz).

e.g. concrete (a combination of aggregate, cement binder and possibly air voids) can be approached in two ways. The first of these is to use a complex material model which expresses the behavior of concrete as a whole within a numerical simulation. Geometrically, there would be no distinction between the aggregate grains and the cement binder. In other words, heterogeneous concrete would be actually treated as a homogeneous material. The second approach is to consider concrete as it really is, i.e. made up of a mix of components. In this case a different material model would be used for the aggregate and cement binder – probably a simpler one. However, this would require the geometric creation of a model that distinguishes between aggregate and cement binder, which could be a demanding task.

In cases when a simple geometry is used with a complex material model that replicates the heterogeneity of the mixture, various optimization, sensitivity and reliability analyses often need to be carried out [1]–[3]. There is a simple reason for this – a complex material model has many inputs which need to be defined. If one chooses to use a complex geometry and relatively simple material models, this problem is avoided. However, the creation of the geometry might be difficult. The complexity of boundary and initial conditions is a chapter in itself [4]–[6]. Again, one can imagine a situation in which the choice of geometry complexity has a decisive impact on the difficulty of solving a numerical simulation and the procedure needed to do that – e.g. an investigation into the fire resistance of a concrete structure [6]. In the vast majority of cases, the basic parameters of the material are available; for instance the thermal expansion or heat capacity of aggregate. However, if it is necessary to determine the thermal characteristics of a mixture, laboratory measurements have to be taken, which is not only a costly but also a time-consuming matter. However, if separate geometries are used for the aggregate and the cement binder, these problems are eliminated completely. It is only necessary to assign each part the aforementioned material properties, which are available in every physics textbook.

The article is divided into two parts in such a way that readers can obtain a better overview of the presented algorithm. The first part of the article deals with the process of creating the geometry of a heterogeneous material – concrete. The selected scale is of a resolution at which the aggregate and cement binder are distinguishable. The whole process is presented as an algorithm which generates geometry from an input photo of real material. As previously mentioned, the use of this approach is motivated by the growing number of inputs demanded by

material models of concrete, particularly with regard to high-speed loading [7], [8]. For example, when the Smoothed Particle Hydrodynamics (SPH) method is used for the calculation, the problem is not the discretization of the investigated domain (i.e. the complexity of the geometry) [9], but rather the difficulty in entering the inputs if complex computational tools are used [10].

Subsequently, in the second part of the article, the generated geometry of concrete – aggregate and cement binder is utilized in the simulation of a cylindrical pressure test using the SPH method. The algorithm in this part shows how the heterogeneity of the material can be enhanced by simply causing the masses of the individual SPH particles to oscillate. There are several options for the use of this numerical heterogeneity. The article shows an application of the oscillation of the masses of SPH particles within the *transition layer* – a layer where aggregate and cement binder are in contact. The conclusion of the article then summarizes the findings and the results of numerical simulations.

## II. THE FIRST PART OF THE ALGORITHM

If a space exists within which a coherent noise function (coherent noise is a type of smooth pseudorandom noise) is able to generate values within a defined range, this suggests that a given set of generated values could have a specific distribution that corresponds to a certain proposed source (input). If the source is a two-dimensional space with values that are either 1 or 0, a cutting plane through the aforementioned noise function space could produce a section possessing values that are identical to those of the source for many criteria.

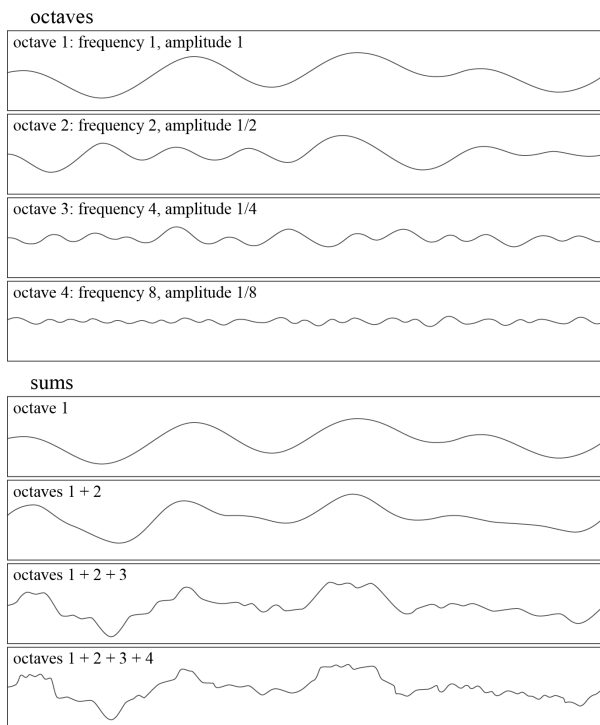


Fig. 1. Creating higher-order Perlin noise by summing the octaves of gradient-based coherent noises.

The coherent noise function can be arbitrary and combinable in any way with other coherent functions, for example Perlin noise [11]. Fig. 1 shows one of the options for the creation of a higher order of coherent noise – due to its self-similar pattern it can be regarded as a fractal. Specifically, it is Perlin noise – a type of coherent noise that is the sum of several coherent-noise functions of ever-increasing frequencies and ever-decreasing amplitudes. The omission of some of the octaves can result in the creation of a very different noise.

With regard to the properties that coherent noise function has:

- 1) entering the same input value (seed) will always return the same output value,
- 2) a small change in the input value (seed) will produce a small change in the output value,
- 3) a large change in the input value (seed) will produce a random change in the output value,

it is possible to create a pattern which corresponds to the source (input) according to the algorithm in Fig. 2.

A real photograph of material can be understood as a surface on which the values of a function can be plotted. The material is thus defined by the type of function employed, and its values. In the case of concrete, aggregate and cement binder can often be recognized in the photograph. The vast majority of photographs are in color, however, and so not suitable for the purpose of analysis. In order to be able to understand a photograph as a function (i.e. data source) with only two values, e.g. aggregate 1 and cement binder 0, the photograph must be adapted via the assignment of colors. This process is depicted in the left part of the diagram in Fig. 2. The right part of the diagram shows the construction of the noise function in such a way that the best possible agreement with the input photo is achieved.

### A. Generation of Spatial Geometry

To enable an easier understanding of the algorithm, the following part of the article illustrates the process of creating the geometry of concrete with various aggregate grain shapes – the first part of the algorithm. Fig. 3 shows the aforementioned left part of the diagram from Fig. 2. The suitable adaptation of the photograph of the material allows the foreground – aggregate (black) and background – cement binder (white) to be distinguished. Black represents 1 values and white 0 values.

A series of analyses follows this adaptation, consisting in the distinguishing of shapes, sizes and the evaluation of the global value  $\Lambda$  – Lacunarity [12], [13], based on the average values  $\lambda_{\epsilon, g}$  determined for each size of the evaluation box with a beginning and orientation as

$$\lambda_{\epsilon, g} = (CV_{\epsilon, g})^2 = \left( \frac{\sigma_{\epsilon, g}}{\mu_{\epsilon, g}} \right)^2 \quad (1)$$

where  $CV$  is the coefficient of variation,  $\sigma$  the standard deviation and  $\mu$  the mean, for pixels per box.

There are also other Lacunarity calculation methods, e.g. those listed in [14]–[17]. However, the values obtained do not differ from the value gained using (1). The analyzed values of the

photograph of the material remain in the computer’s memory and are constantly compared during noise generation. Fig. 4 shows the right part of the diagram from Fig. 2.

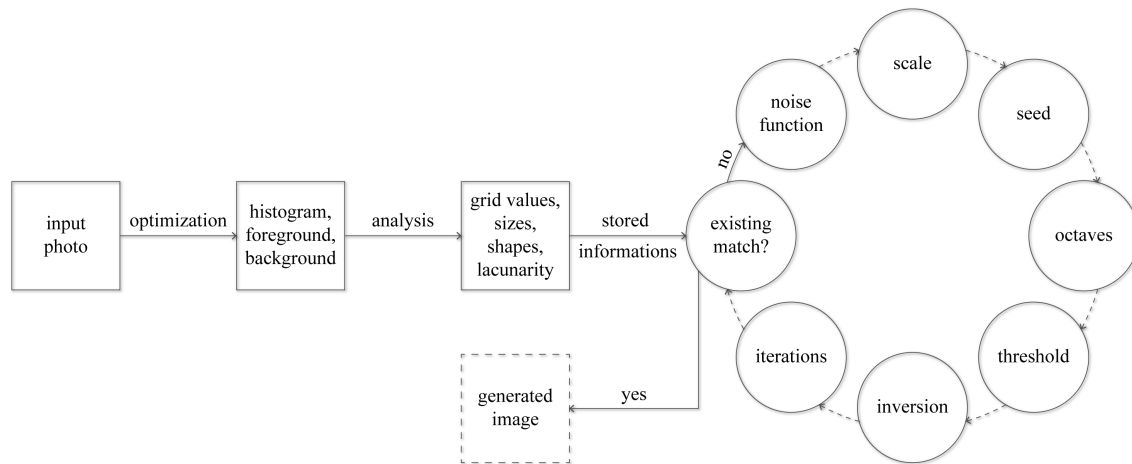


Fig. 2. Diagram of the first part of the algorithm for material structure generation based on an input photo.

The generation and subsequent optimization of noise consists of several different steps. In the first step, a suitable coherent noise function is selected. Function databases are often freely accessible and in many cases include both original and modified noise variants [18]. An example is Perlin noise [11] with applied smoothing of transition borders, which was used in presented example and is shown in Fig. 4.

noise in this stage still has many colors even though it is only in grayscale. By choosing a suitable threshold value, it is possible to say which shades of gray will become black and which, in contrast, will become white – i.e. which will have the values 1 and 0. This choice can have several impacts.

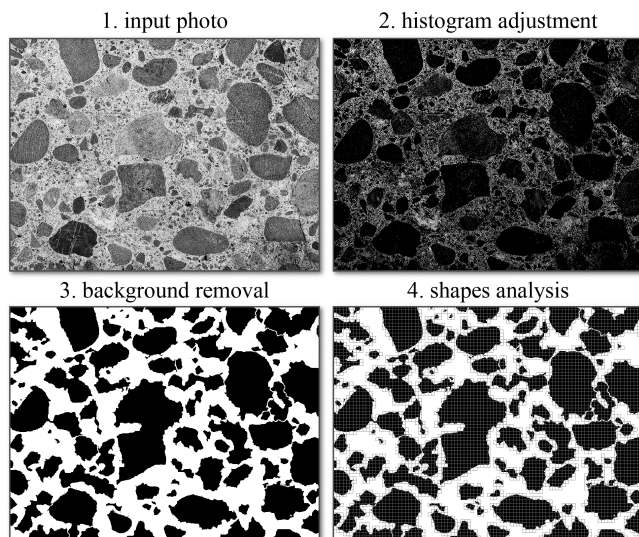


Fig. 3. Preparing the input photo for analysis.

Subsequently, the scale is changed and a suitable seed value selected so that the generated image is as similar to the input photo as possible. In the next step, the algorithm tries to include the shape of the aggregate and possibly its sharpness. As the aggregate in Fig. 3 has relatively sharp edges, the number of included octaves had to be increased, see also Fig. 1. In this stage, shapes approximating those in the input photo were created in a general manner. The next optimization step consists in the use of the *threshold value*, which is related (to a certain degree) to the potential use of color inversion. The generated

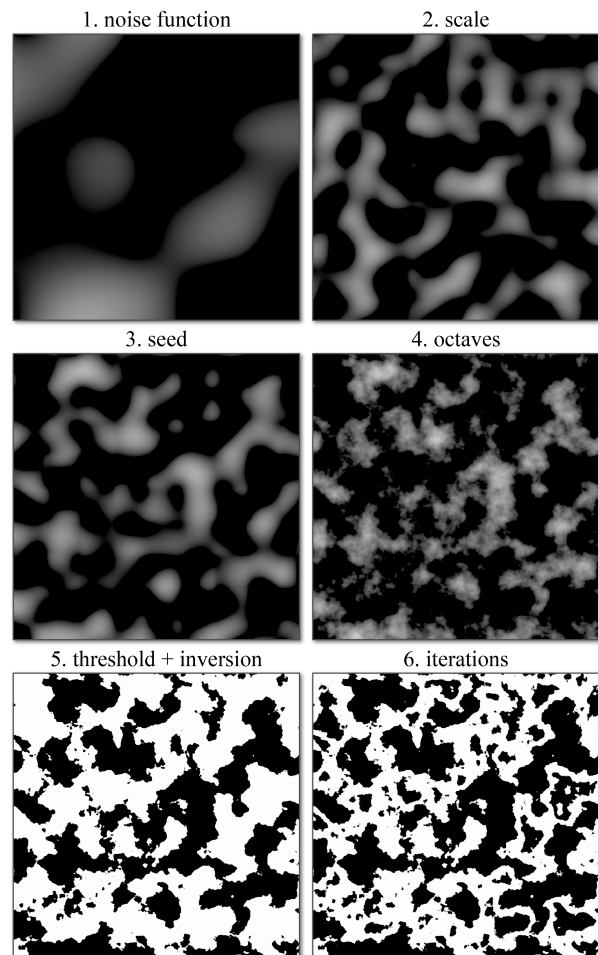


Fig. 4. Generating the structure of the material for comparison with the input photo.

For example, it can, to a certain extent, alter the aggregate size which is specified by the scale value as a priority. Black and white can be inverted if one wishes to determine whether the generated noise could be improved. It should be stated that the threshold value is used for the whole time in the background of the optimization, but at a limited level. The last step of the algorithm is noise iteration. Put simply, with iterations, the noise starts to project itself onto itself and add up in a suitable manner. The obtained effect can represent additionally generated aggregate grains in places where only cement binder was present. If it is subsequently recognized that there is good congruence between the input photo and the generated image, the process of noise generation and its optimization is completed. Fig. 5 shows a more detailed comparison of the input photo and generated image.

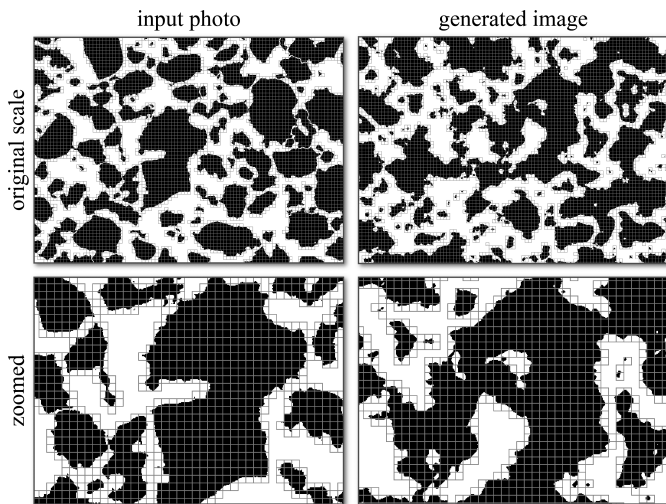


Fig. 5. Comparison of the input photo and the generated image.

### B. Evaluation of Generated Geometry

As previously said, even though only a section of the material was compared, the noise functions can be seen to be spatial. Any changes to the generated section are also projected into the noise space. Both of the generated structures, aggregate and cement binder, are depicted in the form of a cylinder in Fig. 6.

As can be seen from Fig. 6, the spatial geometry of the aggregate as well as the cement binder makes a very realistic and convincing impression. The spatial arrangement of the aggregate and its size were influenced mainly by the choice of noise function, selected scale and seed value. These parameters can thus be considered to be global. The shape itself, the proportions and details of the aggregate were then influenced by the selection of the number of octaves, the threshold value level and the number of iterations. With regard to this fact, these parameters can be considered to be local. It is obvious from what was mentioned that the first part of the algorithm utilizes the descending concept of optimization, which is usual for the majority of optimization algorithms.

### III. THE SECOND PART OF THE ALGORITHM

The created aggregate and cement binder geometry can subsequently be discretized by any numerical method and then

used in simulations with a suitably allocated material model. This procedure can be utilized in practically every numerical method known today, including the SPH method.

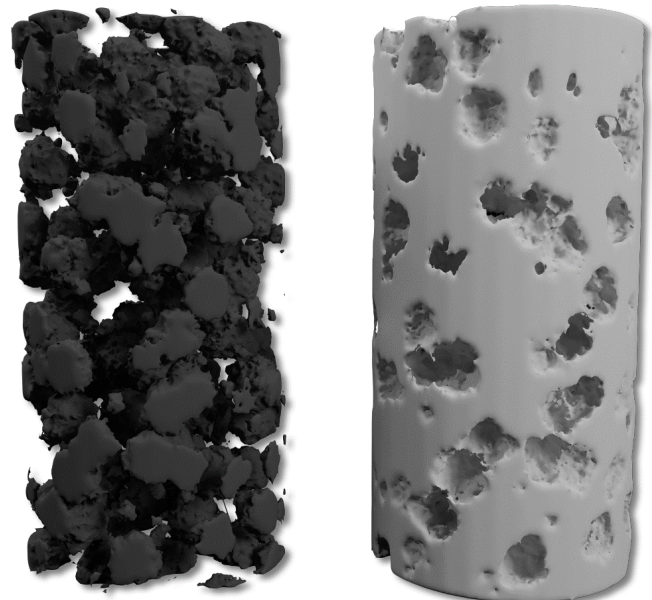


Fig. 6. Generated structure of concrete. From the left: aggregate and cement binder.

With the described procedure, variable results can be obtained (e.g. for cylindrical pressure tests performed on concrete) which will still correspond to those from real experiments. In this case, the *variability* concerns the failure of the concrete cylinder, and the related stress–strain curve. Thanks to this, various sensitivity analyses can be tested.



Fig. 7. Generated structure of the transition layer of concrete.

There is a way to enhance the introduced heterogeneities even further, or bring them even closer to reality. It needs to be pointed out that the whole process is very simple when the SPH method is used. It is all about the use of the layer where aggregate and cement binder are in contact – the transition

layer. The surface of the aggregate may not always be perfectly covered with cement binder, and the process of the solidification and hardening of cement in this area also may not be perfect. This can result in areas on the aggregate where the adhesion of the cement binder may or may not be optimal. In practice, in the case of the SPH method, this means the properties of the particles belonging to this layer require suitable modification.

In order to continue, the spatial geometry of the transition layer needs to be obtained. Again, it can be obtained in several

ways, e.g. by using the geometry of the aggregate or the cement binder. The contact surfaces can be considered to be the midsurface of the transition layer. The spatial geometry or volume of the transition layer can be obtained via a simple symmetrical offset in the direction of the normals of the geometry. The SPH particles which lie within the volume of the transition layer are the aforementioned particles with which the properties will be modified. Fig. 7 shows the transition layer for the already generated aggregate and cement binder geometry.

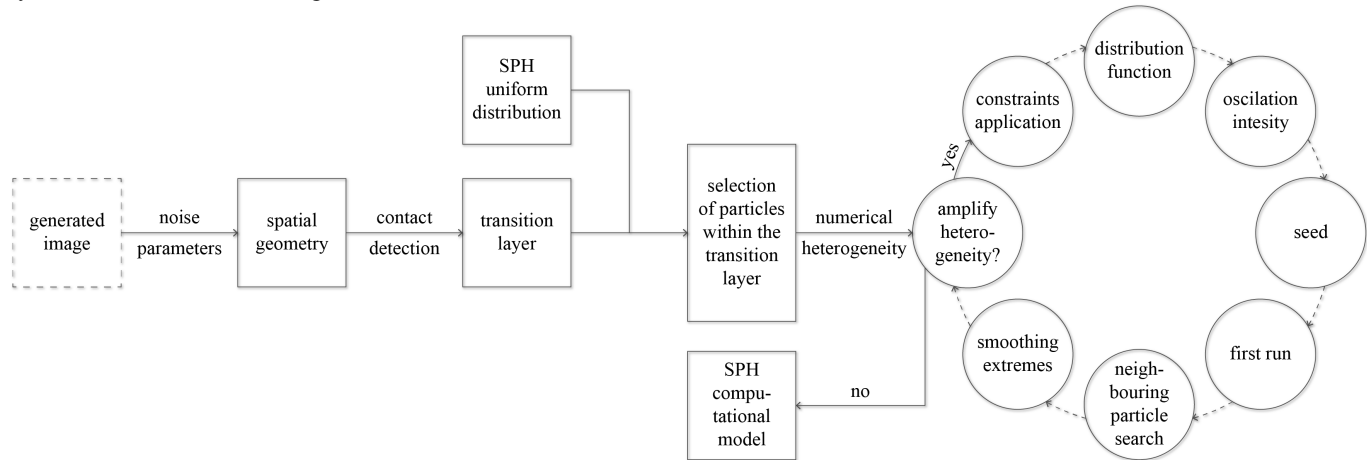


Fig. 8. Diagram of the second part of the algorithm for material structure generation based on an input photo.

#### A. About the SPH Method

The formulation of the SPH method is often divided into two key steps. The first step is the *integral representation* of field functions, and the second is *particle approximation* [19]. Assuming that the finite volume  $\Delta V_j$  is assigned to SPH particle  $j$ , the following relationship applies

$$m_j = \Delta V_j \rho_j \quad (2)$$

where  $m_j$  and  $\rho_j$  are the mass and density of particle  $j$ . The value of the monitored quantity  $f(\mathbf{x}_i)$ , which is the product of integral representation and particle approximation operations, can thus be written as

$$f(\mathbf{x}_i) \approx \sum_{j=1}^N \frac{m_j}{\rho_j} f(\mathbf{x}_j) W(\mathbf{x}_i - \mathbf{x}_j, h) \quad (3)$$

where  $W$  is the smoothing function and  $h$  is the smoothing length defining the influence area of the smoothing function  $W$ . Equation (3) states that the value of a function at particle  $i$  is approximated using the average of those values of the function at all of the particles in the support domain of particle  $i$  weighted by the smoothing function [19].

#### B. SPH Particles Within and Outside the Transition Layer

For an easier understanding of numerical heterogeneity and in order to avoid possible misunderstandings, a prerequisite has been introduced: all particles have the same material model

allocated to them – in other words,  $\rho_j$  is the same for every  $j$  particle. At the same time, in order to eliminate the chance of the occurrence of numerical cracks [20]–[22], the particles are distributed in such a way that they are arranged into a regular grid – in other words,  $\Delta V_j$  is the same for every  $j$  particle. With regard to the above-mentioned facts, it can be concluded that every SPH particle has the same mass  $m_j$  with regard to validity (2). This state can be regarded as the initial state that exists before the creation of the material parameter oscillations themselves, and simultaneously as the next step of the second part of the algorithm. SPH particles outside the transition layer area consequently remain with their initial parameters  $\rho_j$ ,  $\Delta V_j$  and thus also  $m_j$ . SPH particles within the transition layer will have these parameters modified to a certain degree.

#### C. How to Amplify Heterogeneity

Each SPH particle can be considered a Lagrange element with regard to the fact that the mass  $m_j$  allocated to a particle moves together with the particle during the simulation. Also, it can be stated that mass  $m_j$  acts in (3) as a weight coefficient. The higher the  $m_j$  value, the more particle  $j$  is going to influence its surroundings. This information can be utilized very simply to create *numerical heterogeneity* [23].

Numerical heterogeneity can be considered to be an adaptation of the computational model in the sense of the modification of its numerical code or of the numerical method with which the simulation is calculated. Combination is also possible. The following process can be considered a combination of both methods as it essentially modifies the computational model as well as the numerical method. The

modification consists in the introduction of the oscillation of the masses of SPH particles within the transition layer. However, this oscillation will directly precede the compilation of equations (3) for each  $i$  particle. In other words, the oscillation of the weight coefficient occurs directly. Other impacts may include the creation of virtual geometry in the background of the calculation; more information can be found in [23]. The process of creating numerical heterogeneity and also the rest of the second part of the algorithm can be seen in the diagram in Fig. 8.

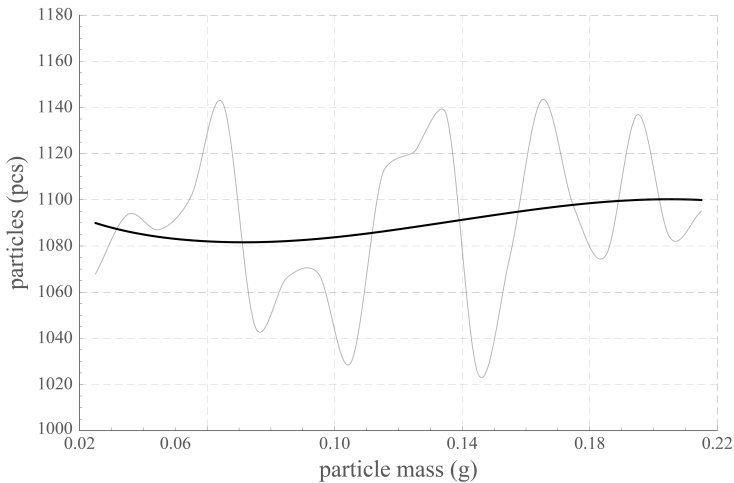


Fig. 9. The mass distribution function generated for particles within the transition layer.

In the first stage of the creation of numerical heterogeneity, constraints must be applied if there are any. These can be, for example, the sum of all modified masses, which has to equal the original sum of unmodified masses. In the next steps, the selection of the statistical distribution of masses and the intensity of oscillations themselves takes place. After the generation of these new masses, or weight coefficients, the evaluation of the smoothness of the transitions of the whole generated field occurs. In other words, the sizes of the differences in oscillations between the neighboring SPH particles are evaluated. If the differences are too great, smoothing of these transitions takes place, thanks to which the simulation is more stable. If the numerical heterogeneity is then evaluated as being sufficient, the computational model is ready. Otherwise, another generated series of oscillations can be added, which further enhances the numerical heterogeneity. The distribution of masses can resemble that shown in Fig. 9, where it is depicted in the form of a histogram interleaved by a curve of a selected statistical distribution.

#### IV. NUMERICAL SIMULATIONS

To illustrate the functionality of the algorithm, static load tests conducted on cylindrical concrete specimens (numerical models or models for short) using controlled displacement were simulated. Stress–strain curves were recorded at the same time. The cylindrical specimens were 300 mm high and 150 mm in diameter. As one of the conditions for the functionality of the introduced algorithm was the regularity of the initial particle

distribution, the cylinders were discretized with 80 particles along the height and 40 particles along the width or depth. The particles were arranged into a regular grid field, not a radial one, and a total of 15 load tests were simulated. The first tested model did not contain any heterogeneities – in the following text, it is referred to as a homogeneous model. The remaining 14 heterogeneous models were created using the described algorithm.

The simulations involved 97,280 SPH particles in total and were performed via the LS-DYNA program [24]. The Continuous Surface Cap Model (CSCM) was chosen as the material model of concrete to be used [25], [26], meaning that material was the same everywhere except for the transition layer where oscillations were included. The CSCM material model has been tested by the authors many times in the past and was selected mainly due to its great ability to capture even complex types of loading, see e.g. [7]–[9], [27]. Table I shows the parameters employed in the simulations.

Table I. The material parameters for the CSCM model.

Mass density, $\rho_c$ ( $\text{kgm}^{-3}$ )	2207
Compressive strength, $f_c$ (MPa)	47
Initial shear modulus, $G$ (GPa)	12.92
Initial bulk modulus, $K$ (GPa)	14.15
Poisson's ratio, $\nu_c$	0.18
Fracture energy, $G_F$ ( $\text{Jm}^{-2}$ )	83.25

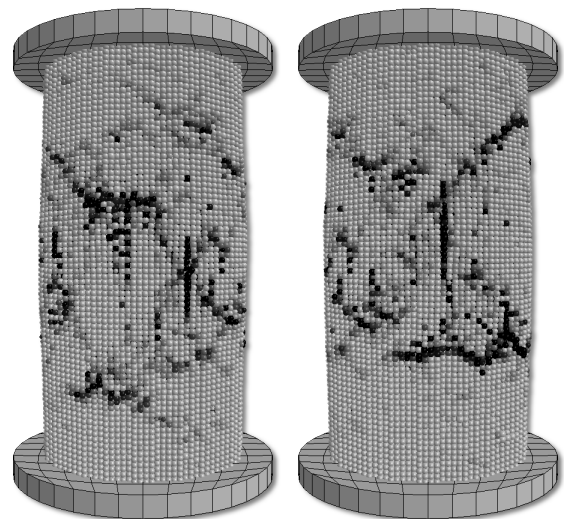


Fig. 10. Failure of two generated models at the end of the pressure test. Light gray particles – undamaged; black particles – damaged.

#### V. RESULTS OF NUMERICAL SIMULATIONS

The aim of the numerical simulations was the creation of variable results which still correspond to those of real experiments as much as possible. The requirement was mainly to obtain variable types of failure and the stress–strain curves which correspond to them. Thanks to the variability of the results, various sensitivity analyses can be tested, a fact which will play an important role in any possible optimization processes. As material structure from 14 different input photos

supplemented with 14 unique mass oscillations was generated for the 14 tested models, there really are differences in the obtained results.

Fig. 10 shows a comparison of the failure of two test models. It is obvious that the failure in each case is similar, yet different. Fig. 11 shows the stress–strain curves. The homogenous model curve is drawn with a thick line.

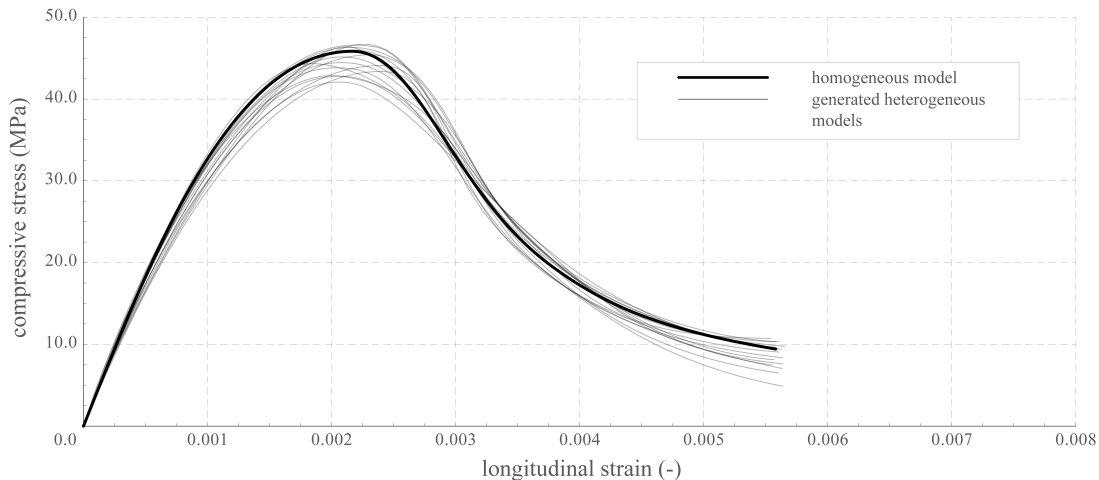


Fig. 11. Stress–Strain curves of homogeneous and generated heterogeneous models.

## VI. CONCLUSIONS

The first part of the article presents the process of creating spatial geometry – material structure of concrete, using an algorithm based on the comparison of an input photo of real material with the generated image of a section cut through a space filled with noise. Using a simple algorithm cycle, in which the optical congruence of the input and generated image are improved thanks to a change in the parameters of the noise functions, the spatial structure of the material is generated in the background of the process. The first part of the article presents the functionality and individual steps of the process using example of the generation of concrete with various aggregate grain shapes.

The second part of the article works with the created geometry and shows how it is possible to enhance the created heterogeneities further in the case of the use of the Smoothed Particle Hydrodynamics method. The creation of a transition layer is explained, as well as the role it plays in numerical simulations. The second part of the algorithm concentrates on the creation of numerical heterogeneity. Again, a simple cycle based on the choice of distribution function and the intensity of the oscillations of material parameters is sufficient for the creation of numerical heterogeneity. Also, numerical simulations of concrete load tests are included in the second part of the article. The functionality of the second part of the algorithm is again supported by results which demonstrate, among other things, a certain variability in the stress–strain curves of the tested numerical models.

The article as a whole presents a procedure which enables signs of heterogeneity to be included in numerical simulations in a very simple way.

It is clear that the heterogeneous models oscillate around this curve. However, the vast majority of the heterogeneous models do not reach the maximum load bearing capacity, i.e. 47 MPa. This can be explained as being due to the high intensity of mass oscillations or insufficient smoothing of the oscillations of the neighboring SPH particles.

## ACKNOWLEDGEMENTS

This outcome has been achieved with the financial support of the project GACR 17-23578S “Damage assessment identification for reinforced concrete subjected to extreme loading” provided by the Czech Science Foundation, and also with the support of the project FAST-J-17-4264 “Experimental and numerical verifications of meshfree methods in cases of dynamically loaded concrete structures” provided by the Brno University of Technology fund for specific university research.

## REFERENCES

- [1] Z. Kala, “Global sensitivity analysis in stability problems of steel frame structures,” *Journal of Civil Engineering and Management*, vol. 22, no. 3, pp. 417–424, 2016.
- [2] Z. Kala, “Sensitivity and Reliability Analyses of Lateral-torsional Buckling Resistance of Steel Beams,” *Archives of Civil and Mechanical Engineering*, vol. 15, no. 4, pp. 1098–1107, 2015.
- [3] Z. Kala, “Reliability analysis of the lateral torsional buckling resistance and the ultimate limit state of steel beams,” *Journal of Civil Engineering and Management*, vol. 21, no. 7, pp. 902–911, 2015.
- [4] J. Kralik, and M. Baran, “Numerical Analysis of the Exterior Explosion Effects on the Buildings with Barriers,” *Applied Mechanics and Materials*, vol. 390, pp. 230–234, 2013.
- [5] J. Kralik, “Safety of nuclear power plants under the aircraft attack,” *Applied Mechanics and Materials*, vol. 617, pp. 76–80, 2014.
- [6] J. Kralik, M. Klabnik, and A. Grmanova, “Probability analysis of a composite steel and concrete column loaded by fire,” *Applied Mechanics and Materials*, vol. 769, pp. 126–132, 2015.
- [7] J. Kala, and M. Husek, “Improved element erosion function for concrete-like materials with the SPH method,” *Shock and Vibration*, vol. 2016, pp. 1–13, 2016.
- [8] J. Kala, and M. Husek, “High speed loading of concrete constructions with transformation of eroded mass into the SPH,” *International Journal of Mechanics*, vol. 10, pp. 145–150, 2016.
- [9] M. Husek, J. Kala, P. Kral, and F. Hokes, “Effect of the support domain size in SPH fracture simulations,” *International Journal of Mechanics*, vol. 10, pp. 396–402, 2016.

- [10] J. Flodr, P. Kałdunski, M. Krejsa, and P. Parenica, "Numerical modelling of clinching process," *Journal of Engineering and Applied Sciences*, vol. 12, pp. 1670–1673, 2017.
- [11] K. Perlin, "An image synthesizer," *ACM SIGGRAPH Computer Graphics*, vol. 19, no. 3, pp. 287–296, 1985.
- [12] T. G. Smith, G. D. Lange, and W. B. Marks, "Fractal methods and results in cellular morphology – dimensions, lacunarity and multifractals," *Journal of Neuroscience Methods*, vol. 69, no. 2, pp. 123–136, 1996.
- [13] R. E. Plotnick, R. H. Gardner, W. W. Hargrove, K. Prestegard, and M. Perlmutter, "Lacunarity Analysis: A General Technique for the Analysis of Spatial Patterns," *Physical Review E*, vol. 53, pp. 5461–5468, 1996.
- [14] R. E. Plotnick, R. H. Gardner, and R. V. O'Neill, "Lacunarity indices as measures of landscape texture," *Landscape Ecology*, vol. 8, no. 3, pp. 201–211, 1993.
- [15] N. E. McIntyre, and J. A. Wiens, "A novel use of the lacunarity index to discern landscape function," *Landscape Ecology*, vol. 15, no. 4, pp. 313–321, 2000.
- [16] A. B. Karperien, *Defining microglial morphology: form, function, and fractal dimension*, Charles Sturt University, 2004, 247 p.
- [17] A. Karperien. (2013). FracLac for ImageJ [Online]. Available: <https://imagej.nih.gov/ij/plugins/fraclac/FLHelp/Introduction.htm>
- [18] P. G. Vivo and J. Lowe. (2015). The Book of Shaders [Online]. Available: <http://www.thebookofshaders.com>
- [19] G. R. Liu, and M. B. Liu, *Smoothed particle hydrodynamics: a meshfree particle method*, New Jersey: World Scientific, 2003, 449 p., ISBN 981-238-456-1.
- [20] J. W. Swegle, D. L. Hicks, and S. W. Attaway, "Smoothed particle hydrodynamics stability analysis," *Journal of Computational Physics*, vol. 16, pp. 123–134, 1995.
- [21] T. Belytschko, Y. Guo, W. K. Liu, and P. Xiao, "A unified stability analysis of meshless particle methods," *International Journal for Numerical Methods in Engineering*, vol. 48, pp. 1359–1400, 2000.
- [22] W. Benz, "Smoothed particle hydrodynamics: a review," in *NATO Workshop*, Les Arcs, France, 1989.
- [23] M. Husek, F. Hokes, J. Kala, and P. Kral, "Inclusion of Randomness into SPH Simulations," *WSEAS Transactions on Heat and Mass Transfer*, vol. 12, pp. 1-10, 2017.
- [24] Livermore Software Technology Corporation (LSTC), "LS-DYNA theory manual," LSTC, Livermore, California, USA, 2017.
- [25] Y. D. Murray, "User's manual for LS-DYNA concrete material model 159," FHWA-HRT-05-062, 2007.
- [26] Y. D. Murray, A. Abu-Odeh, and R. Bligh, "Evaluation of concrete material model 159," FHWA-HRT-05-063, 2006.
- [27] P. Kral, J. Kala, and P. Hradil, "Verification of the elasto-plastic behavior of nonlinear concrete material models," *International Journal of Mechanics*, vol. 10, pp. 175–181, 2016.